Locational Marginal Pricing for Flexibility and Uncertainty with Moment Information

Haoyuan Wang, *Student Member, IEEE,* Zhaohong Bie, *Senior Member, IEEE,* and Hongxing Ye, *Senior Member, IEEE*

***Abstract*—The continuous growth of variable renewable integration has greatly increased uncertainty and variability in the power system, resulting in unprecedentedly high demand for flexibility. Recently, there has been much attention in the power industry to manage the flexibility and uncertainty via market mechanisms. This paper presents a novel approach to jointly clearing energy, reserve, and uncertainty with moment information based on distributionally robust chance constraints (DR-CC). Locational marginal prices (LMP) are derived for both energy and reserve. Uncertainty is modeled with statistical moments of historical forecast errors, and uncertainty marginal prices (UMP) are defined to reflect the marginal cost of uncertainty following the cost-causation principle. The congestion cost of reserve trading is explicitly modelled, and is shown to fully cover financial transmission right (FTR) underfunding. We show that the proposed mechanism guarantees revenue adequacy and provides appropriate incentives for efficient operation and investment. Case studies are carried out to illustrate the impact of the proposed market scheme, and its feasibility is demonstrated on a testbed system based on a real-world 1934-bus grid.**

***Index Terms*—Uncertainty Marginal Price, Flexibility, Locational Marginal Price, Distributionally Robust**

NOMENCLATURE

Indices

t	Index for time intervals.
i, l	Indices for buses and lines.
j, k	Indices for uncertainty sources.
i_k	Bus index of uncertainty source k.

Variables

$\tilde{d}_{i,t}, d_{i,t}$	Real and expected load of bus i.
$\tilde{r}_{i,t}, r_{i,t}$	Real and expected renewable power output of bus i.
$g_{i,t}$	Generator output of bus i.
$u_{i,t}$	UC decision variable for bus i.
$R_i^{\text{up}}, R_i^{\text{dn}}$	Up/Down reserve by bus i.
$P_{i,t}^{\text{inj}}$	Net power injection at bus i.
$P_{l,t}$	Power flow on branch l.
$P_{l,\text{sec}}^{\text{up}}, P_{l,\text{sec}}^{\text{dn}}$	Up/Down transmission security margins.
$\boldsymbol{\xi}$	Vector of uncertain deviations.
$\beta_{i,k}$	Balancing factor of i for uncertainty k.
$x_{l,k}$	Sensitivity of branch power flow l regarding uncertain deviation k.
$\lambda_{i,t}$	Energy LMP for i.
$\eta_{R,i}^{\text{up}}, \eta_{R,i}^{\text{dn}}$	Up/Down reserve LMP for i.
$\nu_{l,k}^{\text{con}}$	Reserve congestion cost on branch l due to uncertainty k.
$C_{\xi,i,k}$	Uncertainty payment by k for flexibility at i.
$E_{R,i,k}$	Reserve payment to i for balancing k.
$F_{l,i,k}^{\text{con}}$	Reserve congestion cost on branch l for mitigating uncertainty k from i.

Constants:

$\boldsymbol{\Gamma}$	Covariance matrix of uncertainty.
$\boldsymbol{\Gamma}^{\frac{1}{2}}$	Decomposition of covariance matrix that satisfies $(\boldsymbol{\Gamma}^{\frac{1}{2}})^T\boldsymbol{\Gamma}^{\frac{1}{2}} = \boldsymbol{\Gamma}$.
$\mathbf{P}$	Correlation matrix of uncertainty.
μ_k, σ_k	Mean and standard deviation of uncertain deviation k.
$\rho_{k,j}$	Correlation coefficient between k and j.
ϵ_i, ϵ_l	Risk tolerance for bus i and branch l.
$\text{SF}_{l,i}$	Load shift factor of branch l for bus i.
$\boldsymbol{D}_\xi$	Incidence matrix for uncertainty.
$\boldsymbol{\Xi}$	Uncertainty set for distributions of $\boldsymbol{\xi}$.

I. INTRODUCTION

As more countries are targeting net-zero carbon emission goals, the penetration of renewable energy has been fast growing in power systems worldwide, leading to a high level of uncertainty and variability [1]. This poses a serious challenge to the safe and reliable operation of power systems, and more flexibility is needed to maintain the real-time power balance [2].

In deregulated power markets, an important source of flexibility is reserve, which is typically regarded as an ancillary service (AS) and usually co-optimized with energy in the security-constrained unit commitment (UC) and economic dispatch (ED) problems [3]. The reserve requirement is often decided by the independent system operator (ISO), and the reserve price is obtained together with the energy price as a byproduct of the ED [4]. However, the system-wide reserve constraint may lead to deliverability issues [5], [6], as the cheapest reserve may not be able to delivered to certain buses due to transmission congestion. Some markets mitigate the deliverability problem by applying zonal pricing [7]. However, zonal prices do not fully resolve the deliverability problem, and may also lead to fairness issues, as nodal prices are not readily divided into zones with clear boundaries in a meshed network [8].

In current markets, AS cost is often allocated to energy consumers as fixed costs or additional tariffs. For example, the PJM market assigns regulation obligation to each load serving entity (LSE) based on its load-ratio share in the region [9]. The additional AS used by variable energy resources (VERs) is paid by energy consumers rather than VER owners. VER

Corresponding author: Hongxing Ye.

H. Wang, Z. Bie, and H. Ye are with the Department of Electrical Engineering, Xi'an Jiaotong University, Xi'an, Shaanxi 710049 China (e-mail: why662@stu.xjtu.edu.cn; zhbie@mail.xjtu.edu.cn; yehxing@xjtu.edu.cn)

owners thus lack incentives to mitigate their generation uncertainty. Such practice cannot accurately reflect the uncertainty impact on system operation, and may distort the price signal.

This paper aims to provide a market scheduling and nodal pricing approach that co-optimizes energy and flexibility, providing proper incentives via marginal prices for both flexible resources and uncertainty sources.

There is rich literature on reserve scheduling with uncertainty in power system operation. Among them, a scenario-based stochastic programming (SP) approach is used in [10] for committing reserves with high penetrations of wind power. To further mitigate risks, robust optimization (RO) is applied in [11] to minimize loss under the worst scenario. RO guarantees an upper limit for system cost, but may result in over-conservative decisions. A chance constrained (CC) programming approach is employed in [12], [13], leading to a predefined probability of constraint compliance. CC programming allows customization of conservativeness, and can be adjusted for various application scenarios with different reliability requirements. However, the true distribution of uncertainty can be hard to obtain in practice.

In recent years, there has been much discussion on distributionally robust (DR) co-optimization of energy and reserves [14]–[16], which optimizes dispatch against the worst possible probability distribution. In these approaches, knowledge of the underlying distribution is not necessarily required. In the meantime, DR-based approaches can not only better leverage historical data, but also avoid the conservativeness of traditional RO.

Integrating chance constraints into DR approaches, the distributionally robust chance-constrained (DR-CC) model [17]–[21] guarantees the solutions satisfy constraints with a predefined confidence level for any distribution within an ambiguity set. A moment-based DR-CC reserve scheduling model is proposed in [17], [18], resulting in a bilinear matrix inequality (BMI) problem solved by sequentially convex optimization. Reference [19] incorporates demand response, and extends the uncertainty set by considering the uncertain availability of elastic loads. The unit commitment problem is addressed in [20], where the DR chance constraints are reformulated with binary variables and are solved with a column-and-constraint generation (C&CG) algorithm. In [21], a Wasserstein DR-CC optimization method is proposed. A physically-bounded bilinear reformulation is provided, which is solved by an iterative algorithm with guaranteed convergence. Although these works address the reserve scheduling problem with DR-CC models, they do not provide a market mechanism.

More recently, DR or DR-CC based approaches have also been applied to market design. A DR model is proposed in [22] for the scheduling of integrated gas-electricity systems with demand response, and LMPs are generated for both electricity and gas markets. A transactive energy framework is proposed in [23] using a DR model that coordinates the energy trading of micogrids and the distribution system operator (DNO), and reference [24] further considers coupled electrical and gas microgrids. A DR optimal power flow (OPF) model is presented in [25] to not only achieve the day-ahead scheduling and pricing of electrical energy, but also provide incentives for optimizing real-time balancing. These works focus the market design of energy-only markets, and therefore do not resolve the pricing issue of flexibility or uncertainty.

On the other hand, reference [26] proposes a novel framework to price reserves using DR chance constraints. It is expanded further in [27] to incorporate asymmetric balancing policies and derive locational balancing prices. They recover reserve cost from uncertainty sources, and cover multiple cases with different balancing policies. Reference [28] designs a chance-constrained peer-to-peer (P2P) joint energy and reserve market, where prices for both energy and reserve are generated in a distributed fashion using the alternating direction method of multipliers (ADMM) method. Reference [29] further introduces data-driven distributionally robustness, and accounts for three-phase unbalanced microgrids. Although these works offer frameworks for distributionally robust reserve trading, they do not reflect the impact of recourse actions on network constraints. Thus, they cannot guarantee reserve deliverability in network congestion cases.

In order to guarantee the deliverability of reserve and provide proper incentives, researchers have tried to design locational marginal prices for reserve and uncertainty. Uncertainty marginal prices (UMP) are proposed in [5] using robust optimization. The UMPs work as prices for both uncertainty and reserves, which are proven to form a competitive equilibrium and guarantee revenue adequacy. However, the results obtained from robust optimization might be too conservative when the most severe contingencies only occur for a very small probability. The idea of locational pricing is explored in [30] for primary and secondary regulation reserves, where reserve requirements are set as fixed values. In [6], [31], uncertainty locational marginal prices (U-LMP) are designed based on DR-CC OPF. Uncertainty sources are charged for the additional reserve. However, it does not give locational marginal prices for reserve. Chance constraints are adopted in [32] to determine reserve capacities according to uncertainty levels, and Lagrange multipliers are used to define locational prices of variability, but revenue adequacy and uncertainty correlation are not taken into account. A scenario-oriented approach is proposed in [33] to jointly clear energy and reserve and achieve marginal pricing of both. However, it can be difficult to obtain the appropriate scenarios without prior knowledge of the real distribution of uncertainty.

Our work further expands the marginal pricing scheme to both sides of the flexibility market, thus revealing the true values of flexibility and uncertainty. A DR-CC framework is proposed to achieve locational marginal pricing of both reserve and uncertainty using the DR-CC approach. We focus on the economic implications and establish cost-causation relationships between reserve and uncertainty, where the congestion cost of reserve trading is explicitly incorporated into the prices. Revenue adequacy and cost recovery are guaranteed for all market entities, and the individual profit of each reserve provider is maximized in a competitive environment.

Compared with RO approaches, the proposed DR-CC approach leverages information from historical data and is generally less conservative. Furthermore, the conservativeness level can be easily controlled based on risk tolerance. It is also

more tractable and computationally efficient. The tractability is important given the growing number of distributed resources with variable power outputs.

Major contributions of this paper are summarized below.

1 We propose a data-driven market clearing model with uncertainty distribution information. Affine policy is employed in recourse actions. The model provides locational marginal prices (LMPs) for both energy and reserve. We show the price-quantity pairs maximize the profit for energy and reserve providers in a competitive environment.
2 We extend the concept of uncertainty marginal price (UMP) to the case when uncertainty set is not available, and design a novel money flow scheme following cost-causation principle. The congestion cost of reserve trading is explicitly modelled, and is shown to guarantee revenue adequacy.
3 We investigate impacts and incentives of the proposed market mechanism via case studies, and test its feasibility on a 1934-bus provincial system. The discussion could provide insights for researches of uncertainty cost allocation.

II. Market Structure and the Optimization Model

This section describes the basic structure of the market, and provides a DR-CC model for the co-optimization of energy and reserve. The DR chance-constraints help guarantee a predefined probability of constraint compliance, even when the output probability distribution of variable generation is uncertain. The model is recast to a second-order cone programming (SOCP) problem.

Following current practice on pricing, it is assumed that unit commitment solutions are given, and we only focus on ED. The model is readily adjusted to incorporate UC by introducing binary variables [20]. This will result in a mixed-integer SOCP problem, which can be efficiently solved using commercial solvers.

A. Market Organization

In the proposed market, transactions regarding energy, reserve, and uncertainty are carried out among market participants. They are cleared simultaneously in a co-optimization process that generates LMPs for energy and reserve and UMPs for uncertainty. The entities being concerned in each kind of transactions are summarized as below.

- *Energy*: Energy is traded from power producers to loads on a nodal basis. The buyers include inelastic loads represented by the ISO, elastic loads (independent or organized via aggregators), and energy storage in the charging mode. The sellers include dispatchable generators, renewable energy resources (RES), and energy storage when discharging.
- *Reserve*: In order to curb uncertainty of power injections, the ISO procures reserve from flexible resources, including dispatchable generators, demand response of elastic loads, and energy storage. Reserves are cleared by node to account for the impact of congestion on reserve deliverability.
- *Uncertainty*: Under normal operating conditions, we define uncertainty as power deviations caused by imperfect forecasts of inelastic load or renewable power. Uncertainty sources are charged by the ISO for the reserve procured to mitigate their uncertainty, including reserve provision and transmission costs. Specifically, moment information from historical data is used to quantify uncertainty.

Transactions between reserve providers and uncertainty sources are carried out centrally via the ISO. Each uncertainty source pays for the deliverable reserve to balance its variability. The reserve-uncertainty trading is analogous to the energy trading in traditional markets, where energy buyers pay for the energy cost that includes congestion costs.

B. Reserve Definition and Uncertainty Set

The classification and terminology of reserves vary greatly for different markets. In this work, we mainly discuss the regulation reserve, which enables generators to maintain real-time power balance by automatically adjusting their outputs, e.g. by following the automatic generation control (AGC) signals. It should be quickly adjustable within a specified time period, e.g. 10 minutes. Some ISOs also require regulation providers to be able to maintain a prescribed output level for a certain period of time (e.g. 1 hour) [34].

Although this paper focuses on reserves provided by generators, the proposed approach can also be adapted to apply to other flexible resources, such as energy storage or elastic loads, as will be demonstrated in case studies in Section V.

The renewable generation and load may deviate from the forecasts. We formulate the deviations as below.

$$\tilde{r}_{i,t} = r_{i,t} + \Delta r_{i,t} \tag{1}$$

$$\tilde{d}_{i,t} = d_{i,t} + \Delta d_{i,t} \tag{2}$$

where $\tilde{r}_{i,t}$ and $r_{i,t}$ are the real and expected outputs of renewable power source at bus i; $\tilde{d}_{i,t}$ and $d_{i,t}$ are the real and expected power demand at bus i; Δr_i and $\Delta d_{i,t}$ are respectively deviations of renewable power and load.

It is assumed that the means $\boldsymbol{\mu}$ and covariance matrix $\boldsymbol{\Gamma}$ of the uncertainties are known from historical data, and the uncertainty set is defined as the set of all possible probability distributions with the same statistical properties:

$$\Xi = \left\{ \mathbb{P}_\xi \,\middle|\, \begin{matrix} \mathrm{E}(\boldsymbol{\xi}) = \boldsymbol{\mu} \\ \mathrm{E}(\boldsymbol{\xi}^T \boldsymbol{\xi}) = \boldsymbol{\Gamma} \end{matrix} \right\} \tag{3}$$

where $\boldsymbol{\xi} \coloneqq \{\Delta \boldsymbol{d}, -\Delta \boldsymbol{r}\}$ is the uncertainty vector representing deviations from forecasts, with positive values indicating unexpected increase of load (or decrease of generation).

The power deviations in the system are compensated for by reserve providers according to balancing participation factors in (4). An affine policy is used, where reserve providers respond to different buses with different linear factors [6], [35].

$$\Delta g_i = \boldsymbol{\beta}_i^T \boldsymbol{\xi} \tag{4}$$

where $\boldsymbol{\beta}_i$ is the column vector of balancing participation factors, with its kth element $\beta_{i,k}$ indicating the proportion of uncertain deviation ξ_k that is balanced by g_i;

Similarly, the deviation of power on transmission lines are approximated as linear functions in uncertainty $\boldsymbol{\xi}$:

$$\Delta P_l = \mathbf{SF}_l^T(\boldsymbol{B}^T - \boldsymbol{D}_\xi)\boldsymbol{\xi} = \boldsymbol{x}_l^T\boldsymbol{\xi} \tag{5}$$

where ΔP_l is the deviation of power carried by line l; $\mathbf{SF}_l$ is the vector of load shift factors of P_l relative to injected power at each bus; $\boldsymbol{B} \coloneqq [\boldsymbol{\beta}_1, \dots, \boldsymbol{\beta}_i, \dots, \boldsymbol{\beta}_N]^T$ is the matrix of balancing factors; $\boldsymbol{D}_\xi$ is the incidence matrix for uncertainty, with $\boldsymbol{D}_\xi(i,k) = 1$ when uncertainty source k is at bus i; $\boldsymbol{x}_l \coloneqq (\boldsymbol{B} - \boldsymbol{D}_\xi^T)\,\mathbf{SF}_l$ is the sensitivity vector describing how deviations $\boldsymbol{\xi}$ influence power flow change on line l.

C. DR-CC OPF

The co-optimization can be formulated as a DR-CC OPF problem. The co-optimization objective is to minimize the total cost for energy and reserves:

$$\sum_{i,t} C_{i,P}\left(g_{i,t}\right) + \sum_{i}\left(C_{i,R}^{\mathrm{up}}\left(R_i^{\mathrm{up}}\right) + C_{i,R}^{\mathrm{dn}}\left(R_i^{\mathrm{dn}}\right)\right) \tag{6}$$

$C_{i,P}$, $C_{i,R}^{\mathrm{up}}$ and $C_{i,R}^{\mathrm{dn}}$ are cost functions for providing energy $g_{i,t}$, upward reserve $R_{i,t}^{\mathrm{up}}$ and downward reserve $R_{i,t}^{\mathrm{dn}}$ at bus i. The functions are assumed to be quadratic or piecewise-linear.

The optimization is subject to the following constraints, with the corresponding Lagrange multipliers given beside them.

- Power generation and ramping limits:

$$g_{i,t} \le u_{i,t}\, g_i^{\max} - R_i^{\mathrm{up}} \qquad (\nu_{i,t}^{\mathrm{up}}) \tag{7}$$
$$g_{i,t} \ge u_{i,t}\, g_i^{\min} + R_i^{\mathrm{dn}} \qquad (\nu_{i,t}^{\mathrm{dn}}) \tag{8}$$
$$(g_{i,t} - g_{i,t-1}) \le u_{i,t}\mathrm{RU}_i\,\Delta t \qquad (\nu_{i,t}^{\mathrm{RU}}) \tag{9}$$
$$(g_{i,t} - g_{i,t-1}) \ge -u_{i,t}\mathrm{RD}_i\,\Delta t \qquad (\nu_{i,t}^{\mathrm{RD}}) \tag{10}$$
$$0 \le R_i^{\mathrm{up}} \le u_{i,t}\mathrm{RU}_i\,\Delta t_R \qquad (\nu_{R,i}^{\mathrm{RU},0}, \nu_{R,i}^{\mathrm{RU}}) \tag{11}$$
$$0 \le R_i^{\mathrm{dn}} \le u_{i,t}\mathrm{RD}_i\,\Delta t_R \qquad (\nu_{R,i}^{\mathrm{RD},0}, \nu_{R,i}^{\mathrm{RD}}) \tag{12}$$

  where $g_{i,t}$ is the generator output of bus i, $u_{i,t}$ is the UC decision solution, RU_i and RD_i are the upward and downward ramp rates, Δt and Δt_R are the time steps for ED and reserve, respectively.
- Nodal and system-wide power balance constraints:

$$g_{i,t} + r_{i,t} - d_{i,t} = P_{i,t}^{\mathrm{inj}} \qquad (\lambda_{i,t}) \tag{13}$$
$$\sum_i P_{i,t}^{\mathrm{inj}} = 0 \qquad (\lambda_t^{\mathrm{sys}}) \tag{14}$$

  where $d_{i,t}$ is the power demand, $r_{i,t}$ is renewable output, and $P_{i,t}^{\mathrm{inj}}$ is the net power injection at bus i.
- Transmission capacity limits:

$$\sum_i \mathrm{SF}_{l,i} P_{i,t}^{\mathrm{inj}} \ge -P_l^{\max} + P_{l,\mathrm{sec}}^{\mathrm{dn}} \qquad (\nu_{l,t}^{\mathrm{dn}}) \tag{15}$$
$$\sum_i \mathrm{SF}_{l,i} P_{i,t}^{\mathrm{inj}} \le P_l^{\max} - P_{l,\mathrm{sec}}^{\mathrm{up}} \qquad (\nu_{l,t}^{\mathrm{up}}) \tag{16}$$

  where $\mathrm{SF}_{l,i}$ is the (l,i) element of shift factor matrix $\mathbf{SF}$ calculated according to DC power flow equations, and $P_{l,\mathrm{sec}}^{\mathrm{up}}$, $P_{l,\mathrm{sec}}^{\mathrm{dn}}$ are upward and downward transmission security margins reserved for uncertainty, respectively.
- Balancing factor constraints:

$$\sum_i \beta_{i,k} = 1 \qquad (\lambda_{\beta,k}) \tag{17}$$

  This equation ensures that the fluctuation of each uncertainty source is exactly balanced.
- Reserve and transmission security chance constraints:

$$\inf_{\mathbb{P}_\xi \in \Xi} \mathbb{P}_\xi\{R_i^{\mathrm{up}} \ge \boldsymbol{\beta}_i^T\boldsymbol{\xi}\} \ge 1 - \epsilon_i \tag{18}$$
$$\inf_{\mathbb{P}_\xi \in \Xi} \mathbb{P}_\xi\{R_i^{\mathrm{dn}} \ge -\boldsymbol{\beta}_i^T\boldsymbol{\xi}\} \ge 1 - \epsilon_i \tag{19}$$
$$\inf_{\mathbb{P}_\xi \in \Xi} \mathbb{P}_\xi\{P_{l,\mathrm{sec}}^{\mathrm{up}} \ge \boldsymbol{x}_l^T\boldsymbol{\xi}\} \ge 1 - \epsilon_l \tag{20}$$
$$\inf_{\mathbb{P}_\xi \in \Xi} \mathbb{P}_\xi\{P_{l,\mathrm{sec}}^{\mathrm{dn}} \ge -\boldsymbol{x}_l^T\boldsymbol{\xi}\} \ge 1 - \epsilon_l \tag{21}$$

  where $\mathbb{P}_\xi$ represents a probability distribution of the uncertainty $\boldsymbol{\xi}$, from the set of possible distributions Ξ.

The DR chance constraints in (18)-(21) ensure that activation of regulation reserves will respect generation or transmission limits with a probability of $1-\epsilon$ even under the worst possible distribution of uncertain variables. ϵ is a small number indicating the risk level. We assume that the violations of different constraints are independent of each other, and adopt a one-sided approximation [26]. A more rigorous formulation will require the use of two-sided joint chance constraints [36].

D. Reformulations of the DR Chance Constraints

Chance constraint (18)-(19) and (20)-(21) are intractable. As we have established linear relationships between uncertain deviations $\boldsymbol{\xi}$ and system variables Δg_i, ΔP_l, statistical information about Δg_i, ΔP_l can be derived based on uncertainty set Ξ defined in (3). The chance constraint can then be recast into the following second-order cone (SOC) forms [37]. The SOC formulations are sufficient conditions of the original form according to Chebyshev inequality.

$$R_i^{\mathrm{up}} \ge \boldsymbol{\beta}_i^T\boldsymbol{\mu} + z_i\left\|\boldsymbol{\Gamma}^{\frac{1}{2}}\boldsymbol{\beta}_i\right\|_2 \qquad (\eta_{R,i}^{\mathrm{up}}) \tag{22}$$
$$R_i^{\mathrm{dn}} \ge -\boldsymbol{\beta}_i^T\boldsymbol{\mu} + z_i\left\|\boldsymbol{\Gamma}^{\frac{1}{2}}\boldsymbol{\beta}_i\right\|_2 \qquad (\eta_{R,i}^{\mathrm{dn}}) \tag{23}$$
$$P_{l,\mathrm{sec}}^{\mathrm{up}} \ge \boldsymbol{x}_l^T\boldsymbol{\mu} + z_l\left\|\boldsymbol{\Gamma}^{\frac{1}{2}}\boldsymbol{x}_l\right\|_2 \qquad (\nu_{R,l}^{\mathrm{up}}) \tag{24}$$
$$P_{l,\mathrm{sec}}^{\mathrm{dn}} \ge -\boldsymbol{x}_l^T\boldsymbol{\mu} + z_l\left\|\boldsymbol{\Gamma}^{\frac{1}{2}}\boldsymbol{x}_l\right\|_2 \qquad (\nu_{R,l}^{\mathrm{dn}}) \tag{25}$$

$\boldsymbol{\Gamma}^{\frac{1}{2}}$ is a matrix satisfying $(\boldsymbol{\Gamma}^{\frac{1}{2}})^T\boldsymbol{\Gamma}^{\frac{1}{2}} = \boldsymbol{\Gamma}$, whose existence is guaranteed by the positive semi-definiteness of $\boldsymbol{\Gamma}$. Uncertainty margin factors $z_i = \sqrt{\frac{1-\epsilon_i}{\epsilon_i}}$ and $z_l = \sqrt{\frac{1-\epsilon_l}{\epsilon_l}}$ are constants determined by risk tolerance ϵ. Assuming that forecast deviations follow symmetric, unimodal distributions, such factors can be further relaxed as $z_i = \sqrt{\frac{2}{9\epsilon_i}}$ and $z_l = \sqrt{\frac{2}{9\epsilon_l}}$ [38].

Substituting (22)-(25) for (18)-(21), the original DR-CC OPF is essentially reformulated into a SOCP problem (P1):

$$\text{(P1)}\ \min \sum_{i,t} C_{i,P}\left(g_{i,t}\right) + \sum_i \left[C_{i,R}^{\mathrm{up}}\left(R_i^{\mathrm{up}}\right) + C_{i,R}^{\mathrm{dn}}\left(R_i^{\mathrm{dn}}\right)\right]$$

s.t. generation constraints: (7)-(12)

balancing and transmission constraints: (13)-(17)

reformulated DR chance constraints: (22)-(25)

Problem (P1) is efficiently solved by commercial solvers. Its Lagrangian function is provided in Appendix A.

Finally, we note that (22)-(23) will result in identical reserve requirements for both upward and downward reserves when the uncertainty variables have zero means ($\boldsymbol{\mu} = 0$), as reserve providers respond to deviations in both directions alike. This is reasonable for regulation reserves, which compensate for short-term power imbalances. However, if it is desired to allow cleared amounts for upward and downward reserves to differ, an asymmetric affine policy can be used [6], where reserve providers respond to upward and downward uncertain deviations asymmetrically. The formulations will be similar. Here, we stick to the symmetric policy to simplify notations and better illustrate the findings regarding pricing.

III. Efficient Locational Marginal Pricing

In this section, we derive LMPs for energy, reserves, and uncertainty. Their compositions are also analyzed.

A. LMPs for Energy and Reserves

We define LMPs for energy, upward reserve, and downward reserve as their respective shadow prices in (P1), in order to reflect their marginal costs in system operation. They can be obtained according to the following proposition:

Proposition 1: Let $\lambda_{i,t}$ denote dual variable for (13), $\eta^{\mathrm{up}}_{R,i}$ denote dual variable for (22), and $\eta^{\mathrm{dn}}_{R,i}$ denote dual variable for (23) in problem (P1). The locational marginal price for energy is $\lambda_{i,t}$, and the locational marginal prices for upward and download reserves are $\eta^{\mathrm{up}}_{R,i}$ and $\eta^{\mathrm{dn}}_{R,i}$, respectively.

The proof is trivial, and is omitted here.

B. Compositions of Energy and Reserve LMP

Based on the Lagrangian function of (P1) provided in Appendix A, we establish propositions below.

Proposition 2: The locational marginal price for energy consists of two components,

$$\lambda_{i,t} = \lambda^{\mathrm{sys}}_t + \sum_l \mathrm{SF}_{l,i}\big(\nu^{\mathrm{dn}}_{l,t} - \nu^{\mathrm{up}}_{l,t}\big), \tag{26}$$

where λ^{sys}_t is system energy cost, and $\sum_l \mathrm{SF}_{l,i}\big(\nu^{\mathrm{dn}}_{l,t} - \nu^{\mathrm{up}}_{l,t}\big)$ is the congestion cost. λ^{sys}_t, $\nu^{\mathrm{dn}}_{l,t}$, $\nu^{\mathrm{up}}_{l,t}$ are the Lagrange multipliers of constraints (14)-(16), respectively.

Proposition 2 can be proven by taking the Lagrangian partial derivative of $P^{\mathrm{inj}}_{i,t}$ to zero.

Similar results can be obtained for for reserve LMPs. As both upward and downward reserves are functions of the balancing factor $\beta_{i,k}$, their marginal prices are thus coupled.

Proposition 3: Locational marginal prices for reserves can be represented as the marginal cost of compensating for uncertainty k. Particularly, when the mean of uncertain deviation k is zero ($\mu_k = 0$),

$$\eta^{\mathrm{up}}_{R,i} + \eta^{\mathrm{dn}}_{R,i} = \frac{\big\|\boldsymbol{\Gamma}^{\frac{1}{2}}\boldsymbol{\beta}_i\big\|_2}{z_i\,\boldsymbol{\Gamma}_k^T\boldsymbol{\beta}_i}\big(\lambda_{\beta,k} - \sum_l \mathrm{SF}_{l,i}\nu^{\mathrm{con}}_{l,k}\big), \tag{27}$$

where $\lambda_{\beta,k}$ is the system flexibility cost for uncertainty k, and $\sum_l \mathrm{SF}_{l,i}\nu^{\mathrm{con}}_{l,k}$ is the reserve congestion cost. $\nu^{\mathrm{con}}_{l,k}$ is defined as

$$\nu^{\mathrm{con}}_{l,k} \coloneqq \mu_k\big(\nu^{\mathrm{up}}_{R,l} - \nu^{\mathrm{dn}}_{R,l}\big) + \frac{z_l\,\boldsymbol{\Gamma}_k^T\boldsymbol{x}_l}{\big\|\boldsymbol{\Gamma}^{\frac{1}{2}}\boldsymbol{x}_l\big\|_2}\big(\nu^{\mathrm{up}}_{R,l} + \nu^{\mathrm{dn}}_{R,l}\big), \tag{28}$$

where $\lambda_{\beta,k}$, $\nu^{\mathrm{up}}_{R,l}$, $\nu^{\mathrm{dn}}_{R,l}$ are the Lagrangian multipliers of constraints (17) and (20)-(21), respectively.

The proof of Proposition 3 can be found in Appendix B. Equation (27) assumes $\mu_k = 0$ for simplicity. When $\mu_k \neq 0$, the left side of the equation will become a different linear combination of $\eta^{\mathrm{up}}_{R,i}$ and $\eta^{\mathrm{dn}}_{R,i}$.

C. Uncertainty Marginal Prices (UMP)

We now derive marginal prices for uncertainty, which is represented by means ($\boldsymbol{\mu}$) and standard deviations ($\boldsymbol{\sigma}$) of forecast errors for variable generation. We employ the concept of shadow price in duality theory. Uncertainty prices provide incentives for variable power to mitigate their own uncertainty.

As standard deviations $\boldsymbol{\sigma}$ are implicitly represented by the covariance matrix $\boldsymbol{\Gamma}$, we first rewrite $\boldsymbol{\Gamma}$ as

$$\boldsymbol{\Gamma} = (\boldsymbol{\sigma}\boldsymbol{\sigma}^T) \odot \mathbf{P} \tag{29}$$

where $\mathbf{P} \coloneqq \{\rho_{i,j}\}$ is the matrix of Pearson correlation coefficients, and $\odot$ is the operator for element-wise multiplication.

The UMPs are then defined as partial derivatives of the Lagrangian function:

$$\lambda_{\mu,k} \coloneqq \frac{\partial \mathcal{L}}{\partial \mu_k} = \sum_i \big(\eta^{\mathrm{up}}_{R,i} - \eta^{\mathrm{dn}}_{R,i}\big)\beta_{i,k} + \sum_l \big(\nu^{\mathrm{up}}_{R,l} - \nu^{\mathrm{dn}}_{R,l}\big)x_{l,k} \tag{30}$$

$$\lambda_{\sigma,k} \coloneqq \frac{\partial \mathcal{L}}{\partial \sigma_k} = \sum_i \big(\eta^{\mathrm{up}}_{R,i} + \eta^{\mathrm{dn}}_{R,i}\big)\frac{z_i \sum_j \rho_{k,j}\beta_{i,k}\beta_{i,j}\sigma_j}{\big\|\boldsymbol{\Gamma}^{\frac{1}{2}}\boldsymbol{\beta}_i\big\|_2} + \sum_l \big(\nu^{\mathrm{up}}_{R,l} + \nu^{\mathrm{dn}}_{R,l}\big)\frac{z_l \sum_j \rho_{k,j}x_{l,j}x_{l,k}\sigma_j}{\big\|\boldsymbol{\Gamma}^{\frac{1}{2}}\boldsymbol{x}_l\big\|_2} \tag{31}$$

where $\lambda_{\mu,k}$ and $\lambda_{\sigma,k}$ are the marginal prices for μ_k and σ_k, respectively. $x_{l,k}$ represents the kth elements in $\boldsymbol{x}_l$. It is observed that both $\lambda_{\mu,k}$ and $\lambda_{\sigma,k}$ have two components. The first component represents marginal reserve cost for uncertainty source k. The second component stands for transmission reserve cost for uncertain power flow.

Although (30) defines marginal price $\lambda_{\mu,k}$ for the mean μ_k of forecast errors, μ_k can be reduced to zero by adjusting the setpoint of variable power to the expected values in practice. Therefore, we are more concerned with the marginal price $\lambda_{\sigma,k}$ for standard deviation σ_k.

As a side note, (30)-(31) can also give UMPs for buses without uncertainty. In this case, the UMPs are only determined by the correlation ρ for existing uncertainty sources. They can provide price signals for the investment of variable generation.

IV. Market Implication and Incentives

In this section we discuss the relationship between reserve and uncertainty payments, and analyze the reserve congestion costs. The marginal prices are shown to follow the cost-causation principle and provide appropriate incentives for efficient operation and investment. Possible problems in implementation are also discussed.

A. Money Flow Analysis and Reserve Congestion

In the proposed market clearing framework, uncertainty sources pay for the cost of reserves that are used to mitigate their uncertainties.

Based on the LMP definitions, the revenue $E_{R,i}$ for reserve provider at bus i is calculated as

$$\begin{aligned} E_{R,i} &\coloneqq \eta^{\mathrm{up}}_{R,i} R^{\mathrm{up}}_i + \eta^{\mathrm{dn}}_{R,i} R^{\mathrm{dn}}_i \\ &= \sum_k \beta_{i,k} \big(\lambda_{\beta,k} - \sum_l \mathrm{SF}_{l,i} \nu^{\mathrm{con}}_{l,k}\big) \\ &= \sum_k E_{R,i,k}. \end{aligned} \tag{32}$$

Similarly, the uncertainty payment $C_{\xi,k}$ by uncertainty source k is calculated as

$$\begin{aligned} C_{\xi,k} &\coloneqq \lambda_{\mu,k}\mu_k + \lambda_{\sigma,k}\sigma_k \\ &= \sum_i \beta_{i,k} \big(\lambda_{\beta,k} - \sum_l \mathrm{SF}_{l,i_k} \nu^{\mathrm{con}}_{l,k}\big) \\ &= \sum_i C_{\xi,i,k}. \end{aligned} \tag{33}$$

The detailed proof of (32)-(33) can be found in Appendix C.

Equation (32) shows that the reserve payment for bus i can be written as the sum of $E_{R,i,k}$, which represents the part of revenue received by i for mitigating the uncertainty of k. Equation (33) shows that the uncertainty payment by k can be written as the sum of $C_{\xi,i,k}$, which stands for the payment by k for the part of uncertainty mitigated by i.

Comparing (32) and (33), uncertainty payment $C_{\xi,i,k}$ can be interpreted as the reserve payment $E_{R,i,k}$ plus reserve congestion costs on all lines from i to k, i.e.

$$C_{\xi,i,k} = E_{R,i,k} + \sum_l F^{\mathrm{con}}_{l,i,k} \tag{34}$$

$$F^{\mathrm{con}}_{l,i,k} \coloneqq \beta_{i,k}(\mathrm{SF}_{l,i} - \mathrm{SF}_{l,i_k})\nu^{\mathrm{con}}_{l,k}, \tag{35}$$

where $\nu^{\mathrm{con}}_{l,k}$ is as defined in (28), and $F^{\mathrm{con}}_{l,i,k}$ represents the reserve congestion cost on line l for mitigating uncertainty k from i. Similar to the traditional congestion cost in energy trading, reserve congestion cost $F^{\mathrm{con}}_{l,i,k}$ may take both positive and negative values, as reserve trading can both exacerbate and alleviate congestion depending on the route of transmission. The total reserve congestion rent always satisfies that $\sum_{l,i,k} F^{\mathrm{con}}_{l,i,k} \geq 0$, as shown in Appendix D. The implications of the reserve congestion rent will be further explored in the next subsection.

Specifically, when the reserve provider and the uncertainty source are located at the same bus ($i_k = i$), or when there is no congestion ($\nu^{\mathrm{con}}_{l,k} = 0$), congestion cost $\sum_l F^{\mathrm{con}}_{l,i,k}$ is reduced to zero, thus

$$E_{R,i,k} = C_{\xi,i,k} = \beta_{i,k} C_{\xi,k}, \tag{36}$$

which means the reserve revenue is exactly equal to the uncertainty payment. This is fundamentally important for uncertainty mitigation, as it treats uncertainty and reserve equivalently. It gives the market viability for uncertainty sources to mitigate their uncertainty by themselves in operation or investing in flexible resources.

B. Revenue Adequacy and FTR Underfunding

In the energy market, energy prices at generator buses are often lower than those at load buses. The resulting net profit is sometimes called congestion rent, which in many power markets is then redistributed to financial transmission right (FTR) holders based on LMP differences [39], [40]. FTR is a tool to hedge against congestion risks, and also helps provide incentives for optimal transmission expansion [41].

Similarly, the trade of reserve and uncertainty also generates a reserve congestion rent, i.e. the total reserve congestion cost $\sum_{l,i,k} F^{\mathrm{con}}_{l,i,k}$. The activation of reserve for balancing uncertainty requires additional security margins for transmission, as shown in (15)-(16), causing a decrease of energy congestion rent and underfunding of FTR [5]. To resolve this issue, we have the following proposition:

Proposition 4: The total uncertainty payment $\sum C_{\xi,k}$ exactly covers the total reserve payment $\sum E_{R,i}$ and maximum FTR underfunding. In other words, the total congestion rent $\sum_{l,i,k} F^{\mathrm{con}}_{l,i,k}$ exactly covers the maximum FTR underfunding.

The proof is provided in Appendix D. Proposition 4 essentially shows that FTR payments are covered by both energy and reserve congestion rents together. Therefore, the proposed pricing scheme effectively guarantees revenue adequacy.

C. Profit Maximization and Competitive Equilibrium

In order to examine the stability of the market clearing results, in this section we prove that each flexible resource can maximize their individual profits under the specified market conditions. For simplicity, it is assumed that the market is fully competitive and all participants are price takers.

Based on KKT conditions, the energy LMPs for generator buses can be represented as (37):

$$\begin{aligned} \lambda_{i,t} =& \frac{dC_{i,P}(g_{i,t})}{dg_{i,t}} + \nu^{\mathrm{up}}_{i,t} - \nu^{\mathrm{dn}}_{i,t} + \nu^{\mathrm{RU}}_{i,t} - \nu^{\mathrm{RD}}_{i,t} \\ &+ \nu^{\mathrm{RU}}_{i,t+1} - \nu^{\mathrm{RD}}_{i,t+1} \end{aligned} \tag{37}$$

which includes terms for marginal generation costs, output limits $\nu^{\mathrm{up}}_{i,t}$, $\nu^{\mathrm{dn}}_{i,t}$, and ramping limits $\nu^{\mathrm{RU}}_{i,t}$, $\nu^{\mathrm{RD}}_{i,t}$, $\nu^{\mathrm{RU}}_{i,t+1}$, $\nu^{\mathrm{RD}}_{i,t+1}$.

Similarly, reserve LMPs can also be analyzed as marginal costs according to KKT conditions, as shown in (38)-(39).

$$\eta^{\mathrm{up}}_{R,i} = \frac{dC^{\mathrm{up}}_{i,R}(R^{\mathrm{up}}_{i,t})}{dR^{\mathrm{up}}_i} + \sum_t \nu^{\mathrm{up}}_{i,t} + \nu^{\mathrm{RU}}_{R,i} - \nu^{\mathrm{RU},0}_{R,i} \tag{38}$$

$$\eta^{\mathrm{dn}}_{R,i} = \frac{dC^{\mathrm{dn}}_{i,R}(R^{\mathrm{dn}}_{i,t})}{dR^{\mathrm{dn}}_i} + \sum_t \nu^{\mathrm{dn}}_{i,t} + \nu^{\mathrm{RD}}_{R,i} - \nu^{\mathrm{RD},0}_{R,i} \tag{39}$$

with components for marginal reserve cost, output limits $\nu^{\mathrm{up}}_{i,t}$, $\nu^{\mathrm{dn}}_{i,t}$, and ramping limits $\nu^{\mathrm{RU}}_{R,i}$, $\nu^{\mathrm{RU},0}_{R,i}$, $\nu^{\mathrm{RD}}_{R,i}$, $\nu^{\mathrm{RD},0}_{R,i}$. Generators are incentivized to adjust their reserve provision until marginal costs are equal to local reserve price, unless constrained by generation limits.

Consider generator at bus i. Given clearing prices $\lambda_{i,t}$, $\eta^{\mathrm{up}}_{R,i}$, and $\eta^{\mathrm{dn}}_{R,i}$, its profit maximization problem (P2) is:

$$\begin{aligned}(\text{P2}) \max_{\left(g_{i,t},R_i^{\mathrm{up}},R_i^{\mathrm{dn}}\right)} & \sum_t \lambda_{i,t} g_{i,t} + \eta^{\mathrm{up}}_{R,i} R_i^{\mathrm{up}} + \eta^{\mathrm{dn}}_{R,i} R_i^{\mathrm{dn}} \\ & - \sum_t C_{i,P}\left(g_{i,t}\right) - C^{\mathrm{up}}_{i,R}\left(R_i^{\mathrm{up}}\right) - C^{\mathrm{dn}}_{i,R}\left(R_i^{\mathrm{dn}}\right) \\ \text{s.t.} \quad & (7)-(12)\end{aligned}$$

With a convex objective function and linear constraints, the above problem is convex, and its optimal solution is attained when the KKT conditions are met. In fact, because $\lambda_{i,t}$, $\eta^{\mathrm{up}}_{R,i}$ and $\eta^{\mathrm{dn}}_{R,i}$ are defined as shadow prices, the KKT conditions of the generator profit maximization problem are exactly reflected by price properties (37)-(39). Thus, the market clearing results also constitute an optimal solution to the participant's profit maximization problem.

It is important to note that the above conclusion is dependent on the affine policy employed in reserve activation. In other words, we assume that reserve providers react to system power imbalances automatically in proportion to linear participation factors. This is a practical assumption, as regulation reserve employs similar strategies in AGC systems [42]. Indeed, when reserve deployment does follow the affine policy, the market clearing results actually form a competitive partial equilibrium [43], where no participant participant has incentive to deviate from the dispatch.

It is noted the competitive equilibrium is based on the assumption that all participants are price takers. In practice, market power is a legitimate concern. Reserve providers may deliberately bid higher than their true costs, in order to raise prices and earn more profits. The actual equilibrium reached will push total system costs higher than the optimal solution.

Although real-world markets are often not fully competitive, the result presented in this subsection is still important. It essentially proves that, with enough competition, market equilibrium will coincide with the system optimal operating point. This guarantees practicality under a baseline situation, and offers system operators a viable option to improve market efficiency. As will be shown in the case study, the impact of market power is limited when the system has sufficient flexible resources available. When flexibility is scarce, the large flexible resource owners will have relatively high market power. It in fact may provide incentive investment for flexible resources, and in turn alleviates the impact of market power. Other measures limiting market power include broader market participation, and better market oversight and regulations.

D. Data Driven Strategy and Market Fairness

The uncertainty set defined in the proposed market clearing scheme does not have clear-cut boundaries. Rather, it is only based on statistical properties, i.e., means and covariances of forecast errors. In other words, the proposed method is a data-driven one. The market clearing results rely heavily on uncertainty set Ξ and risk tolerance level ϵ. The Ξ is obtained from historical data, and can be updated with new observations. Meanwhile, ϵ has an explicit meaning, and can be chosen according to reliability requirements. Therefore, the pricing results generated in this way have better explanatory power, reducing the arbitrariness of traditional methods.

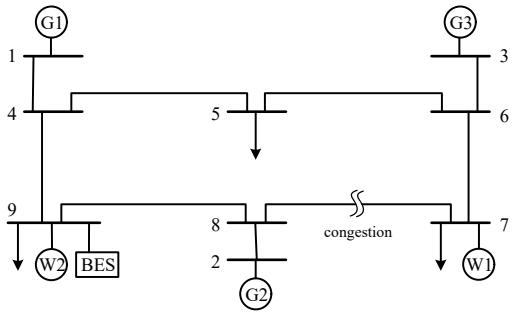

Fig. 1. Modified IEEE 9-bus Power System

To ensure fairness and efficiency, it is ISO's responsibility to maintain a dataset of uncertainty sources, including expected forecast errors, their variances and correlation. It should also be regularly updated. ISOs record the reported forecasts and realizations of variable generation. These records can then be used to reassess the uncertainty levels periodically, e.g. once per year. This provides incentives for uncertainty sources to improve forecasting technology and reduce uncertainty.

Another factor directly affecting market clearing results is distributionally robustness. Within the proposed method, it is possible to achieve robustness for all possible distributions of forecast error. The conservativeness of the results can be further reduced when additional information about the real distribution is available. For example, from empirical results in [44], [45], it can be observed that wind power forecast errors largely follow symmetrical unimodal distributions. Thus, the uncertainty margin factors can be set smaller values according to [38]. In the meantime, the ISO could update their reserve requirements as more data is accumulated in operation.

V. Case Study

The proposed scheme is tested in 3 case studies. A modified IEEE 9-bus system is used to present the basic market clearing results and implications, including a comparison with scenario-based and robust approaches. Then, unit commitment is considered in the IEEE 30-bus system to explore the stability of pricing and the impact of demand response. Finally, feasibility of the proposed market clearing scheme is justified on a testbed based on a 1934-bus provincial system in China.

A. Modified IEEE Nine-Bus System

1) Test Case Description: The proposed scheme is implemented in a modified IEEE 9-bus system, with three generators, two wind farms, and a total peak load of 700 MW.

To investigate the impact on flexible resources, a battery energy storage (BES) system (30 MW/100 MWh) is added. For simplicity, charging/discharging efficiency of the BES system is assumed to be 100%. As continuation time of regulation reserve is very short, the impact of reserve activation on the BES state of charge (SOC) is not taken into account. The one-line diagram of the system is shown in Fig. 1. The parameters of flexible resources are listed in Table I and II.

TABLE I
PARAMETERS OF GENERATORS

#	Bus	P^{max}	P^{min}	RU	RD	a_2	a_1	a_0
G1	1	250	50	125	125	0.1100	5.0	150
G2	2	300	60	150	150	0.0850	1.2	600
G3	3	270	54	135	135	0.1225	1.0	335

P^{max}, P^{min}: maximum/minimum power output (MW)
RU, RD: up/down ramp rate (MW/h)
generation cost: $a_2P^2+a_1P+a_0$ ($)

TABLE II
PARAMETERS OF THE BES

#	Bus	P^{max}	P^{min}	E^{max}	E^{min}	b_1	b_0
BES	9	30	-30	100	10	0.1	0

P^{max}, P^{min}: maximum power output/input (MW)
E^{max}, E^{min}: maximum/minimum energy storage (MWh)
charging/discharging cost: $b_1|P|+b_0$ ($)

Major uncertainty sources are the two wind farms with total capacity of 270 MW. The standard deviation of forecast error is set at 5% of the average output. Forecast error of non-dispatchable load is neglected. All deviations are assumed to be averaged 0. The confidence levels are set to 99.75% for reserve adequacy, and 99% for transmission security chance constraints. Furthermore, in order to analyze the impact of network congestion, the capacity of line 7-8 is deliberately reduced to 100 MW. It could be the case when the line is under maintenance and needs to operate below the designed capacity.

2) Market Clearing Results: Fig. 2 shows the market clearing results of energy, upward reserve, and downward reserve for generator and BES buses in 24 hours. According to Fig. 2, energy prices at selected buses are the same from hour 0 to 9, but diverge greatly from hour 10 to 22. It indicates congestion of line 7-8 occurs from hour 10 to 22. Reserve prices largely show the same patterns. It is noted that marginal reserve prices at BES bus varies violently. Another interesting observation is that upward and downward reserve prices at the BES bus show opposite trends. For example, in hour 7, the upward reserve price reaches its valley \$5.0/MW while downward reserve price attains its peak \$7.7/MW. This is because the costs for BES reserve provision are dependent on its current charging/discharging status. As the network is congested, reserve demanded at bus 9 is largely provided by the BES, which is also located bus 9. Therefore, the reserve prices at bus 9 are largely set by BES marginal costs as well. In the meantime, it also indicates that the proposed pricing mechanism is able to reflect the true value of the flexible resources, even when congestion occurs.

By analyzing the cleared price/quantity pairs, several interesting results are observed for this case. First, BES accounts for almost 1/3 of total cleared reserves, although its installed capacity is less than 5% of total generation capacity. BES tends to be used as a reserve provider due to its flexibility. Second, prices for upward reserves (averaged \$6.3/MW) are slightly higher than those for downward reserves (averaged

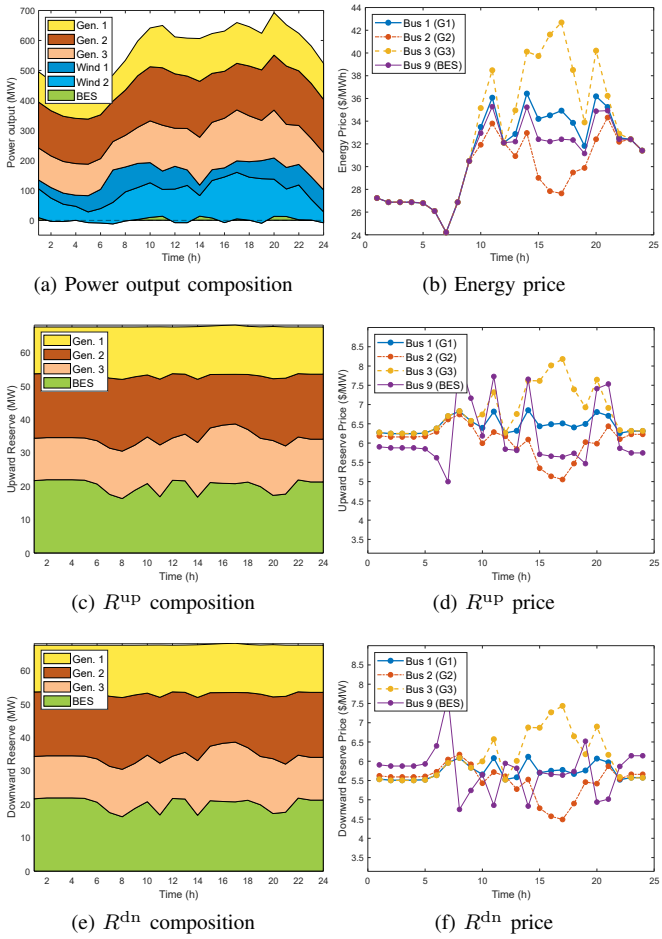

(a) Power output composition (b) Energy price

(c) R^{up} composition (d) R^{up} price

(e) R^{dn} composition (f) R^{dn} price

Fig. 2. Market clearing results

\$6.0/MW). One of the reasons is that upward reserves often incur higher energy costs. Third, reserve prices, ranging \$4.5-8.3/MW, are much lower than energy prices, which are between \$24.2/MWh to \$42.7/MWh.

Fig. 3 shows UMP values (for standard deviation σ) with and without BES in different colors. The color bar shows the price range for both cases. Without BES, the highest UMP \$185/MW is attained in hour 17 at bus 7. Bus 8 has the lowest UMP \$97/MW at hour 16. By introducing BES, the UMPs are reduced in general. For example, the UMP in hour 17 is decreased by \$32/MW (\$28/MW=\$185-153/MW) at bus 7. It indicates that adding less-expensive flexible resources can effectively lower the reserve prices. In both cases, UMPs for the wind farm buses (7 and 9) are the highest. UMPs at bus 2 and 8 are the cheapest, as G2 has the capability to provide reserves to them. However, due to the congestion of line 7-8, G2's less-expensive reserve cannot be delivered to bus 7. That results in high UMP at bus 7. The UMPs at bus 7 and 8 are close in the morning and midnight, but diverges significantly in the afternoon. That is because more flexible resources have to be called for mitigating the uncertainty in the afternoon.

3) Revenue Adequacy and Economical Analysis: To examine economical implications of the DR-CC marginal pricing scheme for flexible resources, cost-revenue analysis for market participants is carried out before and after the integration of

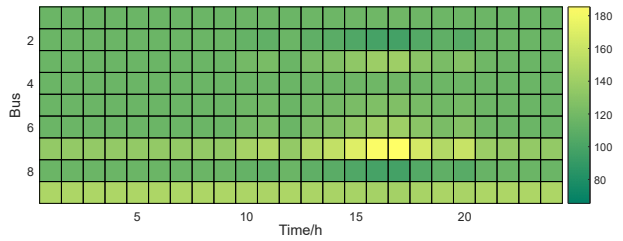

(a) UMPs without BES

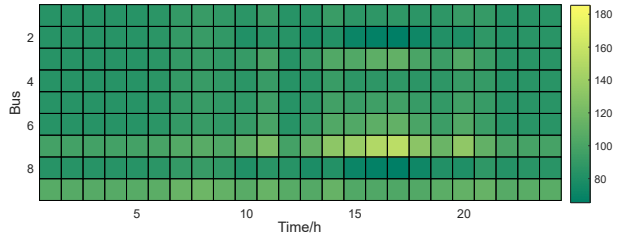

(b) UMPs with BES

Fig. 3. UMPs (for σ) without and with BES integration

TABLE III
REVENUES AND COSTS OF MARKET PARTICIPANTS WITHOUT BES CONNECTION ($\times 10^3$ \$)

	Energy		Reserve		UMP payment	Net profit
	credit	cost	credit	cost		
G1	91.30	-56.41	8.17	-4.53	0	38.33
G2	121.15	-77.39	10.27	-5.69	0	48.25
G3	105.96	-62.58	8.06	-4.41	0	46.82
W1	45.76	0	0	0	-10.17	35.59
W2	72.50	0	0	0	-16.87	55.63
Load	-446.29	0	0	0	0	-446.29
ISO	9.62		-26.50		27.04	10.16

FTR credit: \$10,160

BES. The results are shown in Table III and Table IV.

Comparing Table III and IV, we see that the integration of BES reduces profits for generators by about 2.8%-6.2%, but raises profits for renewables by 7.4%-7.5%. The cheaper flexibility from BES means reserves can be procured at a lower cost. On one hand, it reduces uncertainty payments by renewables. On the other hand, other generators lose part of the reserve revenue. As the BES is mostly dispatched for

TABLE IV
REVENUES AND COSTS OF MARKET PARTICIPANTS FOR BES-CONNECTED CASE ($\times 10^3$ \$)

	Energy		Reserve		UMP payment	Net profit
	credit	cost	credit	cost		
G1	91.09	-56.31	4.27	-2.44	0	36.46
G2	119.83	-76.72	5.23	-3.00	0	45.27
G3	106.70	-62.96	4.45	-2.51	0	45.54
BES	0.40	-0.02	5.75	-3.40	0	2.72
W1	46.08	0	0	0	-7.86	38.22
W2	72.34	0	0	0	-12.51	59.83
Load	-446.77	0	0	0	0	-446.77
ISO	10.34		-19.70		20.36	11.00

FTR credit: \$11,000

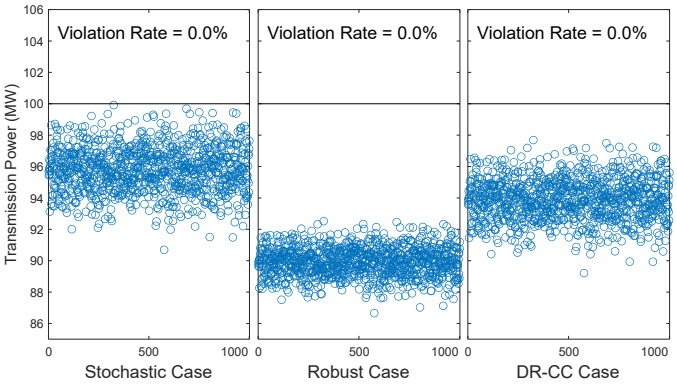

Fig. 4. Monte Carlo sampling of transmission power on Line 7-8 under Gaussian distribution

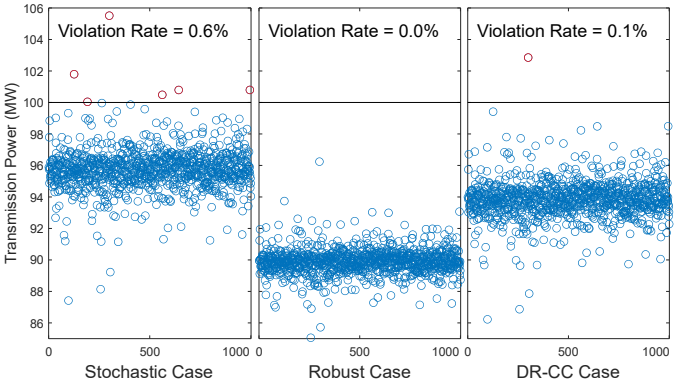

Fig. 5. Monte Carlo sampling of transmission power on Line 7-8 under Student's t distribution ($\nu = 3$)

reserve provision instead of peak shaving, most of its profit (\$2,720) comes from reserve payments instead of arbitrage, which accounts for only \$380. Both cases also validate revenue adequacy, as net profits for the ISO exactly cover the FTR credits (\$10,160 in Table III and \$11,000 in Table IV).

4) Comparison with Stochastic and Robust Approaches: In order to justify the use of the DR-CC approach, the proposed method are compared with the traditional scenario-based and robust optimization approaches. More specifically, three test cases are performed, each with a different approach to system generation and transmission constraints.

- Stochastic case, where the constraints are satisfied for a selected sample of stochastic scenarios.
- Robust case, where the constraints are guaranteed under the worst possible realization of uncertain deviations. The robust model used is as described in [35].
- DR-CC case, where the constraints are only violated with a sufficiently low probability, even under the worst possible distribution of uncertain deviations.

TABLE V
TOTAL OPERATION COST UNDER DIFFERENT APPROACHES ($\times 10^3$ \$)

	Stochastic Case	Robust Case	DR-CC Case
Total Cost	207.47	212.21	207.70

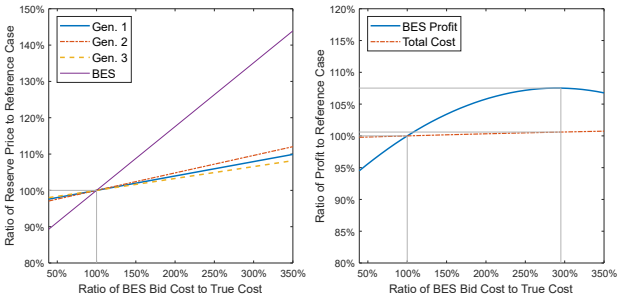

(a) Upward reserve prices (b) Strategic profit and system cost

Fig. 6. Market clearing results with strategic bidding of BES

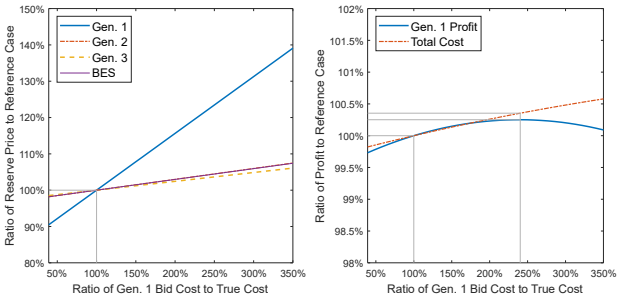

(a) Upward reserve prices (b) Strategic profit and system cost

Fig. 7. Market clearing results with strategic bidding of G1

The robustness of the three approaches are tested using Monte Carlo simulation with 1000 randomly generated samples. Particularly, power flow simulation results on the congested line (Line 7-8) are illustrated in Fig. 4 and Fig. 5. Power deviations of uncertainty sources are sampled according to Gaussian distribution in Fig. 4 and Student's t distribution (with $\nu = 3$) in Fig. 5. In both cases, the sampled uncertain deviations have the same means and standard deviations.

The advantages of the DR-CC approach can be observed by comparing the Monte Carlo simulation results with total costs of the three cases as listed in Table V. The stochastic case has the lowest cost, and can also ensure security under the Gaussian distribution, with zero violation of transmission constraints in 1000 scenarios. However, the violation rate rises to 0.6% when uncertainty takes Student's t distribution, which has a longer "tail" and varies to a greater range. On the other hand, the robust case guarantees compliance of the transmission capacity constraint, by reserving a large security margin and reducing fluctuation of the power flow. In the meantime, system costs rise by \$4,740 compared to the stochastic case. In contrast, the DR-CC case shows a low constraint violation rate of 0.1% in Fig. 5, while the total costs are raised by only \$230 compared with the stochastic case. In practice, the rare instances of transmission limit violation under the DR-CC case can also be avoided with additional intervention of the system operator. This makes the DR-CC approach a good compromise between security and economic efficiency.

5) Impact of Market Power: In this subsection, we investigate the impact of market power, i.e. price-maker model, and illustrate how prices are influenced by the strategic bidding of big players. Specifically, Fig. 6 and Fig. 7 present the market simulation results where the reserve cost bids of BES and G1, respectively, are adjusted while all other participants bid honestly. The results are presented as percentages of values under the reference case, i.e. when all participants bid their true costs.

In both cases, reserve prices and system costs increase linearly as the strategic participant bids higher. The profit of the strategic bidder first increases to a peak value, but then starts to decline as less amount of reserve is provided by it.

As big players, BES and G1 each provide as much as 20-30% of reserves under the reference case (see Fig. 2). However, as shown in Fig. 6 and Fig. 7, their influence on total system costs are limited. When either of them raises reserve bids to optimize their own profits, system costs are only increased by 0.59% and 0.35%, respectively.

Although G1 has a much higher power generation capacity, BES is more flexible. Therefore, the BES can better increase its profit in the reserve market by bidding strategically, and have a higher impact on system costs. For example, at the optimal bidding point, BES can make as much as 7.5% additional profit, while a less flexible resource like G1 can only increase its own profit by 0.25%.

In summary, market power does have an impact on the market outcome. However, the impact is limited when there are alternative flexible resources available. As discussed in Section IV, this can be achieved with broader market participation, or better regulation. Moreover, allowing more flexible resources to make more profit can also encourage investment when there is a lack of flexible capacity in the early stages of the market.

B. IEEE 30-Bus System

1) Case Description: In this part, simulations are conducted with a modified IEEE 30-Bus system. The purpose is to examine the stability and robustness of the proposed market clearing mechanism, especially when UC is taken into account. The test system has three wind power stations with a combined capacity of 90 MW, and a total peak load of 425 MW, of which 5% is elastic load that can participate in the reserve market with demand response.

2) Sensitivity Analysis: A series of SCUC and SCED optimization problems are solved while the total reserve capacity demand is increased from 0 to over 90 MW, which can be achieved by gradually increasing system uncertainty level, or by equivalently lowering risk tolerance. The test result is illustrated in Fig. 8, showing the amount of reserves provided by each generator, and the reserve prices at their buses. The impact of elastic load participation is examined by comparing results with and without demand response of elastic loads.

According to Fig. 8, under both cases, as the total reserve requirement is raised, the cleared quantities and prices for each flexible resource increase accordingly in a piecewise-linear pattern. The turning points occur when more expensive reserves are required or a new unit is committed. For example, in Fig. 8 (c), when the upward reserve requirement is set to 17 MW, the turning point shows an increase in gradient of the reserve price curve. It indicates that G1 and G2, which are

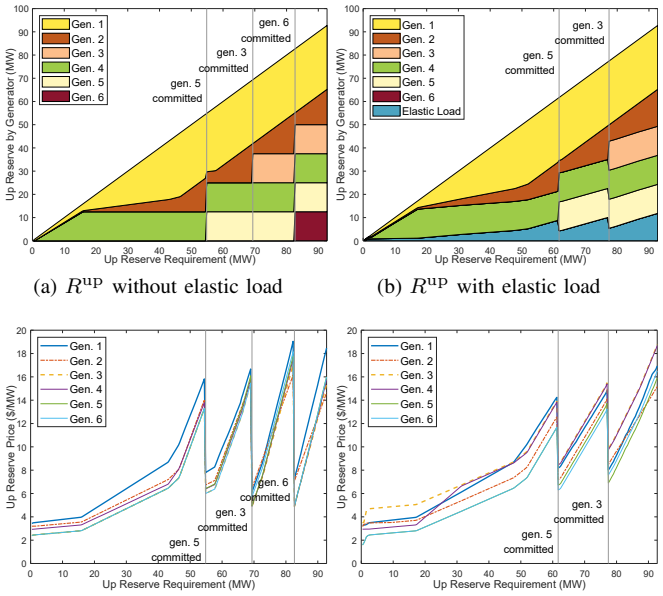

(a) R^{up} without elastic load (b) R^{up} with elastic load

(c) R^{up} prices without elastic load (d) R^{up} prices with elastic load

Fig. 8. Reserve clearing results with increasing total demand

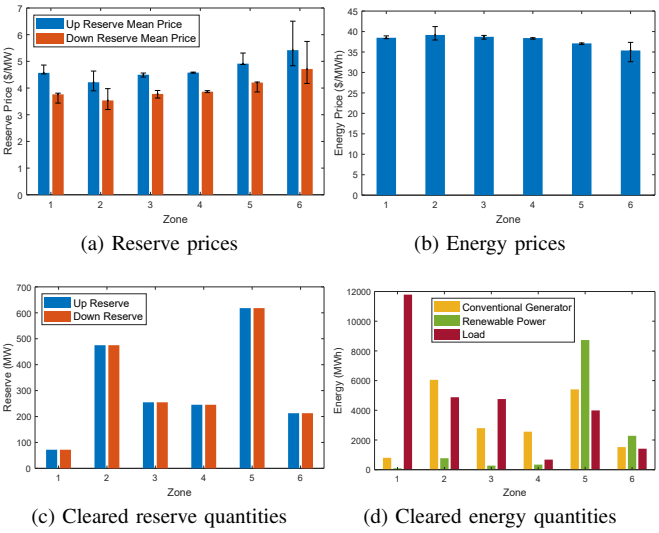

(a) Reserve prices (b) Energy prices

(c) Cleared reserve quantities (d) Cleared energy quantities

Fig. 9. Market clearing results for selected zones

more expensive than G4, have become the marginal generators to set the reserve price. On the other hand, when the upward reserve reserve requirement is set to 55 MW, G5 is committed. In this case, the reserve marginal prices fall down abruptly. That is because the newly committed G5 can provide much cheaper reserves.

Fig. 8 (a), (c), (b), and (d) reveal the contribution of elastic loads. Although only accounting for 5% of the total load, elastic loads provided almost 15% of total reserve at the peak. They can also reduce total system cost by lowering reserve prices and avoid or postpone the introduction of new units. For example, in Fig. 8 (c), without elastic load participation, G3 is committed when total reserve requirement reaches 69.4 MW, and the upward reserve price for G1 is \$16.7/MW. In contrast, Fig. 8 (d) shows that elastic loads defer G3 commitment until reserve requirement reaches 77.4 MW, and G1 upward reserve price drops to \$14.8/MW, This shows the value of demand-side flexibility even if only a small proportion of loads are dispatchable.

C. Shaanxi 1934-Bus System

1) Case Description: We test the proposed approach using the data from a Shaanxi system, with 1934 buses and 2415 branches. The system has a peak load of 35.3 GW, installed conventional generator capacity of 37.3 GW, and installed renewable capacity of 20.9 GW. The renewables are mainly located in the north, and line congestion occurs when the power is delivered to load centers in the south. The system is divided to 12 zones, and we assume generators respond to aggregated uncertainty within a zone.

2) Market Clearing Results: Fig. 9 shows the market clearing results for several zones. In Fig. 9a and 9b, color bars stand for the average reserve and energy prices, with top line marking the maximum price and bottom line marking the minimum price in a zone. It is observed that reserve and energy prices show opposite patterns. For example, Zone 2 has the lowest average reserve price, \$4.2/MW. In contrast, Zone 2 has the highest average price for energy, \$39.2/MWh. Meanwhile, Zone 6 has the highest average reserve price, \$6.4/MW, and the lowest average energy prices, \$35.4/MWh).

Fig. 9c and 9d shows the cleared quantities for reserve and energy, respectively. Zone 6 has the most cleared renewables while Zone 2 has more conventional generators. With the price and quantity results, it is safe to draw the conclusion that the renewable can reduce the energy cost, but also increase the reserve price, as it demands for more flexibility.

On the other hand, we observe that Zone 5 and 6 have large differences between the minimum and maximum prices. For example, the maximum upward reserve price is around \$6.8/MW, and the lowest one is around \$4.6/MW in Zone 5. It indicates the line congestion occurs within Zone 5 and 6.

VI. Conclusion

This paper proposes a market clearing model, and defines locational marginal prices for energy, regulation reserve, and uncertainty. The market clearing model leverages the historical data, and employs distributionally robust chance constraints to guarantee reserve deliverability under uncertainty. The proposed prices explicitly describe marginal values of flexibility and uncertainty, including the congestion cost of reserve transmission. Money flow analysis shows that uncertainty and flexibility are treated equivalently. Fair incentives are provided to both flexible resources and uncertainty sources for their optimal operation and investment. Uncertainty sources are encouraged to curb their variability, e.g. by improving forecast techniques, or investing in flexibility. System revenue adequacy is also guaranteed.

Possible future research topics can include equilibrium analysis in a not fully competitive environment, and market designs that allow broader participation of novel flexible resources from the demand side. A more inclusive electricity market

can help mitigate the impact of increasing uncertainty in the system, and facilitate the transformation of the power system for a greener future.

Appendix A
Lagrangian Function for Problem (P1)

$$
\begin{aligned}
&\mathcal{L}\left(g,P,R,\beta,\lambda,\eta,\nu\right)\\
=&\sum_t\sum_i C_{i,P}\left(g_{i,t}\right)+\sum_i\Big(C^{\mathrm{up}}_{i,R}\left(R^{\mathrm{up}}_i\right)+C^{\mathrm{dn}}_{i,R}\left(R^{\mathrm{dn}}_i\right)\Big)\\
&+\sum_t\sum_i\nu^{\mathrm{up}}_{i,t}\left(R^{\mathrm{up}}_i+g_{i,t}-u_{i,t}\,g^{\max}_i\right)\\
&+\sum_t\sum_i\nu^{\mathrm{dn}}_{i,t}\left(R^{\mathrm{dn}}_i-g_{i,t}+u_{i,t}\,g^{\min}_i\right)\\
&+\sum_t\sum_i\nu^{\mathrm{RU}}_{i,t}\left(g_{i,t}-g_{i,t-1}-u_{i,t}\mathrm{RU}_i\,\Delta t\right)\\
&+\sum_t\sum_i\nu^{\mathrm{RD}}_{i,t}\left(g_{i,t-1}-g_{i,t}-u_{i,t}\mathrm{RD}_i\,\Delta t\right)\\
&+\sum_i\nu^{\mathrm{RU}}_{R,i}\left(R^{\mathrm{up}}_i-u_{i,t}\mathrm{RU}_i\,\Delta t_R\right)-\sum_i\nu^{\mathrm{RU},0}_{R,i}R^{\mathrm{up}}_i\\
&+\sum_i\nu^{\mathrm{RD}}_{R,i}\left(R^{\mathrm{dn}}_i-u_{i,t}\mathrm{RD}_i\,\Delta t_R\right)-\sum_i\nu^{\mathrm{RD},0}_{R,i}R^{\mathrm{dn}}_i\\
&+\sum_t\sum_i\Big(\lambda_{i,t}\big(d_{i,t}-g_{i,t}-r_{i,t}+P^{\mathrm{inj}}_{i,t}\big)-\lambda^{\mathrm{sys}}_t P^{\mathrm{inj}}_{i,t}\Big)\\
&+\sum_t\sum_l\nu^{\mathrm{up}}_{l,t}\Big(P^{\mathrm{up}}_{l,\mathrm{sec}}+\sum_i\mathrm{SF}_{l,i}P^{\mathrm{inj}}_{i,t}-P^{\max}_l\Big)\\
&+\sum_t\sum_l\nu^{\mathrm{dn}}_{l,t}\Big(P^{\mathrm{dn}}_{l,\mathrm{sec}}-\sum_i\mathrm{SF}_{l,i}P^{\mathrm{inj}}_{i,t}-P^{\max}_l\Big)\\
&+\sum_k\lambda_{\beta,k}\Big(1-\sum_i\beta_{i,k}\Big)\\
&+\sum_i\eta^{\mathrm{up}}_{R,i}\left(z_i\left\|\boldsymbol{\Gamma}^{\frac{1}{2}}\boldsymbol{\beta}_i\right\|_2+\boldsymbol{\beta}_i^T\boldsymbol{\mu}-R^{\mathrm{up}}_i\right)\\
&+\sum_i\eta^{\mathrm{dn}}_{R,i}\left(z_i\left\|\boldsymbol{\Gamma}^{\frac{1}{2}}\boldsymbol{\beta}_i\right\|_2-\boldsymbol{\beta}_i^T\boldsymbol{\mu}-R^{\mathrm{dn}}_i\right)\\
&+\sum_l\nu^{\mathrm{up}}_{R,l}\left(z_l\left\|\boldsymbol{\Gamma}^{\frac{1}{2}}\boldsymbol{x}_l\right\|_2+\boldsymbol{x}_l^T\boldsymbol{\mu}-P^{\mathrm{up}}_{l,\mathrm{sec}}\right)\\
&+\sum_l\nu^{\mathrm{dn}}_{R,l}\left(z_l\left\|\boldsymbol{\Gamma}^{\frac{1}{2}}\boldsymbol{x}_l\right\|_2-\boldsymbol{x}_l^T\boldsymbol{\mu}-P^{\mathrm{dn}}_{l,\mathrm{sec}}\right)
\end{aligned}
$$

Appendix B
Proof of Proposition 3

With the Lagrangian function of (P1) defined in Appendix A, the reserve LMPs can be calculated by taking the partial derivatives of $\beta_{i,k}$ to zero.

$$
\begin{aligned}
\frac{\partial\mathcal{L}}{\partial\beta_{i,k}}=&-\lambda_{\beta,k}+\frac{z_i\,\boldsymbol{\Gamma}_k^T\boldsymbol{\beta}_i}{\left\|\boldsymbol{\Gamma}^{\frac{1}{2}}\boldsymbol{\beta}_i\right\|_2}\big(\eta^{\mathrm{up}}_{R,i}+\eta^{\mathrm{dn}}_{R,i}\big)\\
&+\sum_l\mathrm{SF}_{l,i}\frac{z_l\,\boldsymbol{\Gamma}_k^T\boldsymbol{x}_l}{\left\|\boldsymbol{\Gamma}^{\frac{1}{2}}\boldsymbol{x}_l\right\|_2}\big(\nu^{\mathrm{up}}_{R,l}+\nu^{\mathrm{dn}}_{R,l}\big)\\
&+\mu_k\big(\eta^{\mathrm{up}}_{R,i}-\eta^{\mathrm{dn}}_{R,i}\big)+\mu_k\sum_l\mathrm{SF}_{l,i}\big(\nu^{\mathrm{up}}_{R,l}-\nu^{\mathrm{dn}}_{R,l}\big)\\
=&0
\end{aligned}
\tag{40}
$$

The above equation can be rearranged to get

$$
\begin{aligned}
&\Big(1+\frac{\mu_k\left\|\boldsymbol{\Gamma}^{\frac{1}{2}}\boldsymbol{\beta}_i\right\|_2}{z_i\,\boldsymbol{\Gamma}_k^T\boldsymbol{\beta}_i}\Big)\eta^{\mathrm{up}}_{R,i}+\Big(1-\frac{\mu_k\left\|\boldsymbol{\Gamma}^{\frac{1}{2}}\boldsymbol{\beta}_i\right\|_2}{z_i\,\boldsymbol{\Gamma}_k^T\boldsymbol{\beta}_i}\Big)\eta^{\mathrm{dn}}_{R,i}\\
&\qquad=\frac{\left\|\boldsymbol{\Gamma}^{\frac{1}{2}}\boldsymbol{\beta}_i\right\|_2}{z_i\,\boldsymbol{\Gamma}_k^T\boldsymbol{\beta}_i}\big(\lambda_{\beta,k}-\sum_l\mathrm{SF}_{l,i}\nu^{\mathrm{con}}_{l,k}\big),
\end{aligned}
\tag{41}
$$

where $\nu^{\mathrm{con}}_{l,k}$ is as defined in (28).

When $\mu_k=0$, (41) is simplified to (27). Thus, Proposition 3 is proven.

Appendix C
Derivation of Reserve and Uncertainty Payments

We first derive the reserve payment (32). By taking partial derivative for $\beta_{i,k}$ of the Lagrangian function, we have

$$
\begin{aligned}
\frac{\partial\mathcal{L}}{\partial\beta_{i,k}}=\lambda_{\beta,k}-\sum_l\mathrm{SF}_{l,i}\nu^{\mathrm{con}}_{l,k}-\frac{z_i\,\boldsymbol{\Gamma}_k^T\boldsymbol{\beta}_i}{\left\|\boldsymbol{\Gamma}^{\frac{1}{2}}\boldsymbol{\beta}_i\right\|_2}\big(\eta^{\mathrm{up}}_{R,i}+\eta^{\mathrm{dn}}_{R,i}\big)\\
-\mu_k\big(\eta^{\mathrm{up}}_{R,i}-\eta^{\mathrm{dn}}_{R,i}\big)\quad=\ 0.
\end{aligned}
\tag{42}
$$

The complementary conditions for (22)-(23) dictate that

$$
\begin{aligned}
\eta^{\mathrm{up}}_{R,i}R^{\mathrm{up}}_i&=\eta^{\mathrm{up}}_{R,i}\big(\boldsymbol{\beta}_i^T\boldsymbol{\mu}+z_i\left\|\boldsymbol{\Gamma}^{\frac{1}{2}}\boldsymbol{\beta}_i\right\|_2\big)\\
&=\sum_k\eta^{\mathrm{up}}_{R,i}\left(\mu_k+\frac{z_i\,\boldsymbol{\Gamma}_k^T\boldsymbol{\beta}_i}{\left\|\boldsymbol{\Gamma}^{\frac{1}{2}}\boldsymbol{\beta}_i\right\|_2}\right)\beta_{i,k}
\end{aligned}
\tag{43}
$$

$$
\begin{aligned}
\eta^{\mathrm{dn}}_{R,i}R^{\mathrm{dn}}_i&=\eta^{\mathrm{dn}}_{R,i}\big(-\boldsymbol{\beta}_i^T\boldsymbol{\mu}+z_i\left\|\boldsymbol{\Gamma}^{\frac{1}{2}}\boldsymbol{\beta}_i\right\|_2\big)\\
&=\sum_k\eta^{\mathrm{dn}}_{R,i}\left(-\mu_k+\frac{z_i\,\boldsymbol{\Gamma}_k^T\boldsymbol{\beta}_i}{\left\|\boldsymbol{\Gamma}^{\frac{1}{2}}\boldsymbol{\beta}_i\right\|_2}\right)\beta_{i,k}.
\end{aligned}
\tag{44}
$$

Combining results from (42)-(44), we can calculate the total reserve payment for bus i as

$$
\begin{aligned}
E_{R,i}&=\eta^{\mathrm{up}}_{R,i}R^{\mathrm{up}}_i+\eta^{\mathrm{dn}}_{R,i}R^{\mathrm{dn}}_i\\
&=\sum_k\beta_{i,k}\left[\frac{z_i\,\boldsymbol{\Gamma}_k^T\boldsymbol{\beta}_i}{\left\|\boldsymbol{\Gamma}^{\frac{1}{2}}\boldsymbol{\beta}_i\right\|_2}\big(\eta^{\mathrm{up}}_{R,i}+\eta^{\mathrm{dn}}_{R,i}\big)+\mu_k\big(\eta^{\mathrm{up}}_{R,i}-\eta^{\mathrm{dn}}_{R,i}\big)\right]\\
&=\sum_k\beta_{i,k}\big(\lambda_{\beta,k}-\sum_l\mathrm{SF}_{l,i}\nu^{\mathrm{con}}_{l,k}\big)
\end{aligned}
\tag{45}
$$

which is exactly the result in (32).

Next, we derive the uncertainty payment (33). With UMPs $\lambda_{\mu,k}$ and $\lambda_{\sigma,k}$ defined as in (30)-(31), uncertainty payment for k can be directly calculated as

$$
\begin{aligned}
C_{\xi,k}&=\lambda_{\mu,k}\mu_k+\lambda_{\sigma,k}\sigma_k\\
&=\sum_i\beta_{i,k}\,\mu_k\big(\eta^{\mathrm{up}}_{R,i}-\eta^{\mathrm{dn}}_{R,i}\big)\\
&\quad+\sum_l\Big(\sum_i\beta_{i,k}\mathrm{SF}_{l,i}-\mathrm{SF}_{l,i_k}\Big)\mu_k\big(\nu^{\mathrm{up}}_{R,l}-\nu^{\mathrm{dn}}_{R,l}\big)\\
&\quad+\sum_i\beta_{i,k}\big(\eta^{\mathrm{up}}_{R,i}+\eta^{\mathrm{dn}}_{R,i}\big)\frac{z_i\,\boldsymbol{\Gamma}_k^T\boldsymbol{\beta}_i}{\left\|\boldsymbol{\Gamma}^{\frac{1}{2}}\boldsymbol{\beta}_i\right\|_2}\\
&\quad+\sum_l\Big(\sum_i\beta_{i,k}\mathrm{SF}_{l,i}-\mathrm{SF}_{l,i_k}\Big)\big(\nu^{\mathrm{up}}_{R,l}+\nu^{\mathrm{dn}}_{R,l}\big)\frac{z_l\,\boldsymbol{\Gamma}_k^T\boldsymbol{x}_l}{\left\|\boldsymbol{\Gamma}^{\frac{1}{2}}\boldsymbol{x}_l\right\|_2}\\
&=\sum_i\beta_{i,k}\left[\frac{z_i\,\boldsymbol{\Gamma}_k^T\boldsymbol{\beta}_i}{\left\|\boldsymbol{\Gamma}^{\frac{1}{2}}\boldsymbol{\beta}_i\right\|_2}\big(\eta^{\mathrm{up}}_{R,i}+\eta^{\mathrm{dn}}_{R,i}\big)+\mu_k\big(\eta^{\mathrm{up}}_{R,i}-\eta^{\mathrm{dn}}_{R,i}\big)\right]
\end{aligned}
$$

$$+\sum_i \beta_{i,k}\sum_l \mathrm{SF}_{l,i}\nu_{l,k}^{\mathrm{con}} - \sum_l \mathrm{SF}_{l,i_k}\nu_{l,k}^{\mathrm{con}}$$
$$=\sum_i \beta_{i,k}\big(\lambda_{\beta,k} - \sum_l \mathrm{SF}_{l,i_k}\nu_{l,k}^{\mathrm{con}}\big) \quad (46)$$

where the third equality is from the definition of $\nu_{l,k}^{\mathrm{con}}$ in (28), and the fourth equality is from (42) and constraint (17). Thus, uncertainty payment (33) is obtained.

Appendix D
Proof of Proposition 4

We first calculate the difference between total uncertainty payment and total reserve payment, i.e. the total reserve congestion cost. From (32)-(34) and the definition of $\boldsymbol{x}_l$ in (5), we have

$$\sum_k C_{\xi,k} - \sum_i E_{R,i} = \sum_{l,i,k} F_{l,i,k}^{\mathrm{con}} = \sum_l \boldsymbol{x}_l^T \boldsymbol{\nu}_l^{\mathrm{con}} \quad (47)$$

where $\boldsymbol{\nu}_l^{\mathrm{con}}$ is the vector of reserve congestion costs $\nu_{l,k}^{\mathrm{con}}$.

The total reserve congestion rent on the right side of (47) is always non-negative. To see this, first calculate it as

$$\sum_l \boldsymbol{x}_l^T \boldsymbol{\nu}_l^{\mathrm{con}} = \sum_l \nu_{R,l}^{\mathrm{up}}\left(z_l\left\|\boldsymbol{\Gamma}^{\frac{1}{2}}\boldsymbol{x}_l\right\|_2 + \boldsymbol{x}_l^T\boldsymbol{\mu}\right) + \sum_l \nu_{R,l}^{\mathrm{dn}}\left(z_l\left\|\boldsymbol{\Gamma}^{\frac{1}{2}}\boldsymbol{x}_l\right\|_2 - \boldsymbol{x}_l^T\boldsymbol{\mu}\right). \quad (48)$$

Due to complementary slackness, we have

$$\nu_{R,l}^{\mathrm{up}}\left(z_l\left\|\boldsymbol{\Gamma}^{\frac{1}{2}}\boldsymbol{x}_l\right\|_2 + \boldsymbol{x}_l^T\boldsymbol{\mu} - P_{l,\mathrm{sec}}^{\mathrm{up}}\right) = 0 \quad (49)$$
$$\nu_{R,l}^{\mathrm{dn}}\left(z_l\left\|\boldsymbol{\Gamma}^{\frac{1}{2}}\boldsymbol{x}_l\right\|_2 - \boldsymbol{x}_l^T\boldsymbol{\mu} - P_{l,\mathrm{sec}}^{\mathrm{dn}}\right) = 0. \quad (50)$$

According to KKT conditions, the partial derivatives of the Lagrangian $\mathcal{L}$ to $P_{l,\mathrm{sec}}^{\mathrm{up}}$ and $P_{l,\mathrm{sec}}^{\mathrm{up}}$ satisfy that

$$\frac{\partial\mathcal{L}}{\partial P_{l,\mathrm{sec}}^{\mathrm{up}}} = \sum_t \nu_{l,t}^{\mathrm{up}} - \nu_{R,l}^{\mathrm{up}} = 0 \quad (51)$$
$$\frac{\partial\mathcal{L}}{\partial P_{l,\mathrm{sec}}^{\mathrm{dn}}} = \sum_t \nu_{l,t}^{\mathrm{dn}} - \nu_{R,l}^{\mathrm{dn}} = 0. \quad (52)$$

Substituting (49)-(52) into (48), we have

$$\sum_l \boldsymbol{x}_l^T \boldsymbol{\nu}_l^{\mathrm{con}} = \sum_t\sum_l \left(\nu_{l,t}^{\mathrm{up}} P_{l,\mathrm{sec}}^{\mathrm{up}} + \nu_{l,t}^{\mathrm{dn}} P_{l,\mathrm{sec}}^{\mathrm{dn}}\right) \geq 0, \quad (53)$$

i.e. the reserve congestion rent is always non-negative.

On the other hand, the payment to FTR holders is the product of $\mathrm{FTR}_{i\to j}$ quantities and price differences between i and j. With the extra transmission security margins, FTR payments may exceed the total congestion revenue. (54) defines the total FTR underfunding and calculates its upper limit.

$$\begin{aligned}
&\sum_t\sum_{i\to j}(\lambda_{i,t}-\lambda_{i,t})\mathrm{FTR}_{i\to j} - \sum_t\sum_i \lambda_{i,t}(-P_{i,t}) \\
&=\sum_t\sum_{i\to j}\sum_l(\mathrm{SF}_{l,j}-\mathrm{SF}_{l,i})\big(\nu_{l,t}^{\mathrm{up}}-\nu_{l,t}^{\mathrm{dn}}\big)\mathrm{FTR}_{i\to j} \\
&\quad -\sum_t\sum_l\big(\nu_{l,t}^{\mathrm{up}}-\nu_{l,t}^{\mathrm{dn}}\big)P_{l,t} \\
&\leq \sum_t\sum_l\big(\nu_{l,t}^{\mathrm{up}}+\nu_{l,t}^{\mathrm{dn}}\big)P_l^{\max} - \sum_t\sum_l\big(\nu_{l,t}^{\mathrm{up}}-\nu_{l,t}^{\mathrm{dn}}\big)P_{l,t} \\
&\leq \sum_t\sum_l\big(\nu_{l,t}^{\mathrm{up}}P_{l,\mathrm{sec}}^{\mathrm{up}} + \nu_{l,t}^{\mathrm{dn}}P_{l,\mathrm{sec}}^{\mathrm{dn}}\big) \quad (54)
\end{aligned}$$

The first inequality holds due to the FTR simultaneously feasible condition [8]

$$-P_l^{\max} \leq \sum_{i\to j}(\mathrm{SF}_{l,j}-\mathrm{SF}_{l,i})\,\mathrm{FTR}_{i\to j} \leq P_l^{\max}, \quad (55)$$

and the second inequality is guaranteed by transmission capacity limits (15)-(16).

Thus, the maximum FTR underfunding (54) is equal to the total reserve congestion cost (53), which is exactly the surplus of uncertainty payments (47). In other words, revenue adequacy of the proposed market clearing scheme is guaranteed.

References

[1] E. Ela, M. Milligan, A. Bloom, A. Botterud, A. Townsend, and T. Levin, "Evolution of wholesale electricity market design with increasing levels of renewable generation," National Renewable Energy Lab (NREL), Tech. Rep., 9 2014.

[2] B. Mohandes, M. S. E. Moursi, N. Hatziargyriou, and S. E. Khatib, "A review of power system flexibility with high penetration of renewables," *IEEE Transactions on Power Systems*, vol. 34, no. 4, pp. 3140–3155, July 2019.

[3] Y. Tang, C. Luo, J. Yang, and H. He, "A chance constrained optimal reserve scheduling approach for economic dispatch considering wind penetration," *IEEE/CAA Journal of Automatica Sinica*, vol. 4, no. 2, pp. 186–194, April 2017.

[4] M. Shahidehpour, H. Yamin, and Z. Li, *Market operations in electric power systems: forecasting, scheduling, and risk management*. John Wiley & Sons, 2003.

[5] H. Ye, Y. Ge, M. Shahidehpour, and Z. Li, "Uncertainty marginal price, transmission reserve, and day-ahead market clearing with robust unit commitment," *IEEE Transactions on Power Systems*, vol. 32, no. 3, pp. 1782–1795, May 2017.

[6] X. Fang, K. S. Sedzro, H. Yuan, H. Ye, and B.-M. Hodge, "Deliverable flexible ramping products considering spatiotemporal correlation of wind generation and demand uncertainties," *IEEE Transactions on Power Systems*, vol. 35, no. 4, pp. 2561–2574, July 2020.

[7] Y. Chen, P. Gribik, and J. Gardner, "Incorporating Post Zonal Reserve Deployment Transmission Constraints Into Energy and Ancillary Service Co-Optimization," *IEEE Transactions on Power Systems*, vol. 29, no. 2, pp. 537–549, Mar. 2014.

[8] D. R. Biggar and M. R. Hesamzadeh, *The Economics of Electricity Markets*. Wiley-IEEE Press, 2014.

[9] P. Interconnection, *PJM Manual 28: Operating Agreement Accounting*, PJM Interconnection, LLC, December 2020.

[10] A. Papavasiliou, S. S. Oren, and R. P. O'Neill, "Reserve requirements for wind power integration: A scenario-based stochastic programming framework," *IEEE Transactions on Power Systems*, vol. 26, no. 4, pp. 2197–2206, Nov 2011.

[11] N. G. Cobos, J. M. Arroyo, N. Alguacil, and J. Wang, "Robust energy and reserve scheduling considering bulk energy storage units and wind uncertainty," *IEEE Transactions on Power Systems*, vol. 33, no. 5, pp. 5206–5216, Sep. 2018.

[12] H. Wu, M. Shahidehpour, Z. Li, and W. Tian, "Chance-constrained day-ahead scheduling in stochastic power system operation," *IEEE Transactions on Power Systems*, vol. 29, no. 4, pp. 1583–1591, July 2014.

[13] M. Vrakopoulou, B. Li, and J. L. Mathieu, "Chance constrained reserve scheduling using uncertain controllable loads part i: Formulation and scenario-based analysis," *IEEE Transactions on Smart Grid*, vol. 10, no. 2, pp. 1608–1617, March 2019.

[14] W. Wei, F. Liu, and S. Mei, "Distributionally robust co-optimization of energy and reserve dispatch," *IEEE Transactions on Sustainable Energy*, vol. 7, no. 1, pp. 289–300, Jan 2016.

[15] P. Xiong and C. Singh, "Distributionally robust optimization for energy and reserve toward a low-carbon electricity market," *Electric Power Systems Research*, vol. 149, pp. 137–145, 2017.

[16] L. Yao, X. Wang, C. Duan, J. Guo, X. Wu, and Y. Zhang, "Data-driven distributionally robust reserve and energy scheduling over wasserstein balls," *IET Generation, Transmission & Distribution*, vol. 12, no. 1, pp. 178–189, 2018.

[17] Q. Bian, H. Xin, Z. Wang, D. Gan, and K. P. Wong, "Distributionally robust solution to the reserve scheduling problem with partial information of wind power," *IEEE Transactions on Power Systems*, vol. 30, no. 5, pp. 2822–2823, Sep. 2015.

[18] Z. Wang, Q. Bian, H. Xin, and D. Gan, "A distributionally robust coordinated reserve scheduling model considering cvar-based wind power reserve requirements," *IEEE Transactions on Sustainable Energy*, vol. 7, no. 2, pp. 625–636, April 2016.

[19] Y. Zhang, S. Shen, and J. L. Mathieu, "Distributionally robust chance-constrained optimal power flow with uncertain renewables and uncertain reserves provided by loads," *IEEE Transactions on Power Systems*, vol. 32, no. 2, pp. 1378–1388, March 2017.

[20] Z. Shi, H. Liang, and V. Dinavahi, "Data-driven distributionally robust chance-constrained unit commitment with uncertain wind power," *IEEE Access*, vol. 7, pp. 135 087–135 098, 2019.

[21] A. Arrigo, C. Ordoudis, J. Kazempour, Z. De Grève, J.-F. Toubeau, and F. Vallée, "Wasserstein distributionally robust chance-constrained optimization for energy and reserve dispatch: An exact and physically-bounded formulation," *European Journal of Operational Research*, vol. 296, no. 1, pp. 304–322, 2022.

[22] C. He, X. Zhang, T. Liu, and L. Wu, "Distributionally robust scheduling of integrated gas-electricity systems with demand response," *IEEE Transactions on Power Systems*, vol. 34, no. 5, pp. 3791–3803, 2019.

[23] Z. Liu, L. Wang, and L. Ma, "A transactive energy framework for coordinated energy management of networked microgrids with distributionally robust optimization," *IEEE Transactions on Power Systems*, vol. 35, no. 1, pp. 395–404, 2020.

[24] M. Daneshvar, B. Mohammadi-Ivatloo, M. Abapour, S. Asadi, and R. Khanjani, "Distributionally robust chance-constrained transactive energy framework for coupled electrical and gas microgrids," *IEEE Transactions on Industrial Electronics*, vol. 68, no. 1, pp. 347–357, 2021.

[25] Y. Guo, X. Han, X. Zhou, and G. Hug. (2022, Jan.) Incorporate day-ahead robustness and real-time incentives for electricity market design. [Online]. Available: https://arxiv.org/abs/2201.10827

[26] Y. Dvorkin, "A chance-constrained stochastic electricity market," *IEEE Transactions on Power Systems*, vol. 35, no. 4, pp. 2993–3003, July 2020.

[27] A. Gonzalez-Castellanos, A. Hinneck, R. Mieth, D. Pozo, and Y. Dvorkin. (2021, Jun.) Electricity and reserve pricing in chance-constrained electricity markets with asymmetric balancing reserve policies. [Online]. Available: https://arxiv.org/abs/2106.05999

[28] Z. Guo, P. Pinson, S. Chen, Q. Yang, and Z. Yang, "Chance-constrained peer-to-peer joint energy and reserve market considering renewable generation uncertainty," *IEEE Transactions on Smart Grid*, vol. 12, no. 1, pp. 798–809, 2021.

[29] J. Li, M. E. Khodayar, J. Wang, and B. Zhou, "Data-driven distributionally robust co-optimization of p2p energy trading and network operation for interconnected microgrids," *IEEE Transactions on Smart Grid*, vol. 12, no. 6, pp. 5172–5184, 2021.

[30] G. Zhang, E. Ela, and Q. Wang, "Market scheduling and pricing for primary and secondary frequency reserve," *IEEE Transactions on Power Systems*, vol. 34, no. 4, pp. 2914–2924, July 2019.

[31] X. Fang, B.-M. Hodge, E. Du, C. Kang, and F. Li, "Introducing uncertainty components in locational marginal prices for pricing wind power and load uncertainties," *IEEE Transactions on Power Systems*, vol. 34, no. 3, pp. 2013–2024, May 2019.

[32] A. E. Brooks and B. C. Lesieutre, "The validity of a locational marginal price on variable power injections in energy and regulation markets," *International Journal of Electrical Power & Energy Systems*, vol. 121, p. 106092, 2020.

[33] J. Shi, Y. Guo, L. Tong, W. Wu, and H. Sun, "A scenario-oriented approach to energy-reserve joint procurement and pricing," *IEEE Transactions on Power Systems*, pp. 1–1, 2022.

[34] N. DeForest, J. S. MacDonald, and D. R. Black, "Day ahead optimization of an electric vehicle fleet providing ancillary services in the los angeles air force base vehicle-to-grid demonstration," *Applied Energy*, vol. 210, pp. 987–1001, 2018.

[35] H. Ye, "Surrogate Affine Approximation Based Co-Optimization of Transactive Flexibility, Uncertainty, and Energy," *IEEE Transactions on Power Systems*, vol. 33, no. 4, pp. 4084–4096, Jul. 2018.

[36] S. Zymler, D. Kuhn, and B. Rustem, "Distributionally robust joint chance constraints with second-order moment information," *Mathematical Programming*, vol. 137, no. 1, pp. 167–198, February 2013.

[37] G. C. Calafiore and L. El Ghaoui, "On distributionally robust chance-constrained linear programs," *Journal of Optimization Theory and Applications*, vol. 130, no. 1, pp. 1–22, 2006.

[38] L. Roald, F. Oldewurtel, B. Van Parys, and G. Andersson. (2015, Aug.) Security constrained optimal power flow with distributionally robust chance constraints. [Online]. Available: https://arxiv.org/abs/1508.06061

[39] X. Ma, D. Sun, and A. Ott, "Implementation of the pjm financial transmission rights auction market system," in *IEEE Power Engineering Society Summer Meeting,*, vol. 3, 2002, pp. 1360–1365 vol.3.

[40] A. Bykhovsky, D. James, and C. Hanson, "Introduction of option financial transmission rights into the new england market," in *IEEE Power Engineering Society General Meeting, 2005*, 2005, pp. 237–242 Vol. 1.

[41] T. Kristiansen and J. Rosellón, "A merchant mechanism for electricity transmission expansion," *Journal of Regulatory Economics*, vol. 29, no. 2, pp. 167–193, 2006.

[42] H. Bevrani and T. Hiyama, *Intelligent automatic generation control*. CRC press New York, 2011.

[43] A. Mas-Colell, M. D. Whinston, J. R. Green *et al.*, *Microeconomic theory*. Oxford university press New York, 1995, vol. 1.

[44] H. Bludszuweit, J. A. Dominguez-Navarro, and A. Llombart, "Statistical analysis of wind power forecast error," *IEEE Transactions on Power Systems*, vol. 23, no. 3, pp. 983–991, 2008.

[45] J. Wu, B. Zhang, H. Li, Z. Li, Y. Chen, and X. Miao, "Statistical distribution for wind power forecast error and its application to determine optimal size of energy storage system," *International Journal of Electrical Power & Energy Systems*, vol. 55, pp. 100–107, 2014.

Haoyuan Wang (S'18) received the B.S. degree from Xi'an Jiaotong University (XJTU), Xi'an, China. He is pursuing a Ph.D. degree at the Department of Electrical Engineering, XJTU. His research interests concern electricity markets and renewable integration in the power system.

Zhaohong Bie (M'98-SM'12) received the B.S. and M.S. degrees from the Electric Power Department of Shandong University, Jinan, China, in 1992 and 1994, respectively, and the Ph.D. degree from Xi'an Jiaotong University (XJTU), Xi'an, China, in 1998. Currently, she is the Dean of Electrical Engineering College at XJTU. She also serves as the Chair of IEEE Power and Energy Society China Chapter Council. Her main research interests are power system planning and reliability evaluation, integration of the renewable energy, as well as resilient power systems.

Hongxing Ye (SM'17) received the B.S. and M.S. degree from Xi'an Jiaotong University (XJTU), Xi'an, China, and the Ph.D. degree from the Illinois Institute of Technology, Chicago, IL, USA, in 2015, all in Electrical Engineering. He is currently a Professor at XJTU. He was a tenure-track assistant professor at Cleveland State University, Cleveland, USA, before joining XJTU. His research interests include renewable integration, power systems, and data-driven optimization in cyber-physical system.